CHAPTER II

STRUCTURE DETERMINATION OF THE CATALYTIC CORE (DOMAIN B) OF ENVZ

II-1. INTRODUCTION

EnvZ functions in conteracting phosphorylation (histidine kinase)/dephosphorylation (phosphatase) activities. The autophosphorylation of His-243 undergoes in the presence of ATP (Aiba *et al.*, 1989; Forst *et al.*, 1989; Igo and Silhavy, 1988). Moreover, ATP is required for EnvZ-mediated dephosphorylation (i.e. phosphatase activity) of phospho-OmpR and nonhydrolyzable ATP analogues, β, γ-iminoadenosine-5'-triphosphate (AMP-PNP) for an example, can substitute for ATP (Igo *et al.*, 1989). The glycine rich sequence is a conserved feature of many nucleotide binding proteins (Schlosser *et al.*, 1993). Protein kinases that catalyze the phosphorylation of substrate proteins share this sequence and functions as an anchor for ATP.

The cytoplasmic catalytic core of EnvZ (domain B: residues 290-450) shares most of the conserved motifs among the histidine kinases (Figure II-1); Asn-347, Phe-387, and two glycine-rich boxes, DXGXG (G1 box; residues 373-377) and GXG (G2 box; residues 403-405) (for review see Parkinson, 1995). The G1 and G2 boxes are proposed to be involved in nucleotide binding as shown by UV cross-linking experiment with [α-^{32}P] ATP (Ninfa *et al.*, 1993). Interestingly, the mutation study of the conserved Asn-347 to aspartate results in a phenotype in which ATP-dependent autokinase activity is lost and ADP negatively regulates the phosphatase activity of this mutant (Dutta and Inouye, 1996). This implicates the conserved Asn-347 in EnvZ may be involved in defining the ATP binding sites.

The three-dimensional structure of catalytic core of EnvZ or of any other protein histidine kinases have not been determined. The solution structure of domain B is investigated here, therefore, using nucleic magnetic resonance (NMR) spectroscopy in order to obtain the structural features of catalytic region of histidine kinases. In Chapter II, the NMR-derived solution structure of domain B is described and shown to have an α/β sandwich fold.

II-2. MATERIALS AND METHODS

II-2-1. Sample preparation

EnvZ domain B (residues 290-450) was provided by Prof. M. Inouye (University of Medicine and Dentistry of New Jersey, USA). It was expressed and purified as previously described (Egger and Inouye, 1997) except that uniformly ^{15}N- and $^{15}N/^{13}C$-labeled proteins were obtained by using $^{15}NH_4Cl$ and $^{15}NH_4Cl/[^{13}C_6]$-D-glucose as the sole nitrogen and nitrogen/carbon sources in M9 medium, respectively. NMR samples contained 1.0 to 1.5 mM uniformly ^{15}N- or $^{15}N/^{13}C$-labeled, or unlabeled protein in either 95 % H_2O/5% ^2H_2O or 99.996% ^2H_2O containing 20 mM sodium phosphate, 50 mM KCl, 0.5 mM 4-(2-aminoethyl)-benzylsulfonyl fluoride hydrochloride (AEBSF, ICN Pharmaceutical Inc.), 50 μM sodium azide and 5 mM $MgCl_2$ (pH 7.0) with 5 mM unlabeled AMP-PNP (Pharmacia Inc.) or $^{15}N/^{13}C$-labeled AMP-PNP (a gift from Prof. Kainosho, Tokyo Metropolitan University, Tokyo, Japan).

The mass of the EnvZ domain B was confirmed to be the expected molecular weight as determined by light scattering and gel filtration analyses. They indicated that domain B is monomeric in solution (Appendix Table A-1.).

II-2-2. NMR spectroscopy

All NMR spectra were recorded at 25 °C, unless otherwise noted, on a four-channel UNITY 600 spectrometer. All data were processed using the software nmrPipe and nmrDraw (Delaglio *et al.*, 1995), and the data analysis was assisted by the software CAPP and PIPP (Garrett *et al.*, 1991).

Two-dimensional (2D) ^{15}N-^1H HSQC (Kay *et al.*, 1992) and ^1H-^{13}C CT-HSQC (Vuister and Bax, 1992) spectra were recorded with the following numbers of complex points and acquisition times: ^{15}N (F1) 256, 140 ms, ^1H (F2) 512, 64 ms with 16 transients for ^{15}N-^1H HSQC and ^{13}C (F1) 160, 27 ms, ^1H (F2) 384, 48 ms with 64 transients for ^1H-^{13}C CT-HSQC.

The 2D $^1H/^{15}N$ HMQC-J (Kay and Bax, 1990) spectrum was recorded on a UNITY-plus 500 spectrometer with the following numbers of complex points and acquisition times: ^{15}N (F1) 400, 290 ms, ^1H (F2) 512, 64 ms (96 transients).

Slowly-exchanging amide protons were identified by recording a series of gradient-enhanced ^{15}N-^1H HSQC (Kay *et al.*, 1992) experiments at a range of time intervals (21, 43, 75, 105, 285,

330, 920, 2128, and 4125 min.) beginning after exchanging H_2O buffer to ^2H_2O buffer using PD-10 gel filtration column at 4 °C. The spectra were recorded with the following numbers of complex points and acquisition times: ^{15}N (F1) 64, 39 ms, ^1H (F2) 512, 57 ms with 8 transients (total measurement time 17 min.).

The $^{15}N\{^1H\}$ NOE was measured as described (Kay *et al.*, 1989). The spectra with and without the NOE effect were recorded with the following numbers of complex point and acquisition times: ^{15}N (F1) 128, 78 ms, ^1H (F2) 512, 57 ms, 96 transients. Resonance intensities were used to determine the NOE values.

Two-dimensional (Hβ)Cβ(CγCδ)Hδ and (Hβ)Cβ(CγCδCε) experiments (Yamazaki *et al.*, 1993) were recorded with the following numbers of complex points and acquisition times: ^{13}C (F1) 32, 8 ms, ^1H (F2) 512, 64 ms, 224 transients.

Homonuclear 2D NOESY (Jeener *et al.*, 1979) and TOCSY (Braunschweiler and Ernst, 1983) spectrum was recorded with the following numbers of complex points and acquisition times: ^1H (F1) 512, 85 ms, ^1H (F2) 512, 85 ms (48 transients). For the NOESY experiments, mixing time of 100 ms was used. A WALTZ16 (Shaka *et al.*, 1983) sequence was used in the TOCSY experiment with mixing time of 36 ms.

All triple-resonance 3D spectra were recorded on the uniformly $^{15}N/^{13}C$-labeled H_2O sample with the following numbers of complex points and acquisition times: HNCO (Kay *et al.*, 1990), ^{13}CO (F1) 64, 39 ms, ^{15}N (F2) 38, 23 ms, ^1H (F3) 512, 64 ms (16 transients); (HB)CBCACO(CA)HA (Kay, 1993), $^{13}C_{\alpha/\beta}$ (F1) 52, 7.1 ms, ^{13}CO (F2) 64, 39 ms, ^1H (F3) 384, 64 ms (16 transients). The following spectra were recorded on a UNITY-plus 500 spectrometer with the following numbers of complex points and acquisition times: (HB)CBCA(CO)NNH (Grzesiek and Bax, 1992), $^{13}C_{\alpha/\beta}$ (F1) 48, 6.3 ms, ^{15}N (F2) 32, 23 ms, ^1H (F3) 512, 64 ms (28 transients); HNCACB (Wittekind and Mueller, 1993), $^{13}C_{\alpha/\beta}$ (F1) 48, 6.3 ms, ^{15}N (F2) 28, 21 ms, ^1H (F3) 512, 64 ms (48 transients).

A 3D HCCH-TOCSY (Kay *et al.*, 1993) spectrum with mixing time of 14 ms was recorded with the following numbers of complex points and acquisition times: ^1H (F1) 128, 37 ms, ^{13}C (F2)

32, 11 ms, ^{1}H (F3) 416, 52 ms (16 transients). The 3D ^{15}N-edited TOCSY-HMQC (Clore *et al.*, 1991) spectra were recorded on a UNITY-plus 500 spectrometer with the following numbers of complex points and acquisition times: ^{1}H (F1) 128, 21 ms, ^{15}N (F2) 32, 23 ms, ^{1}H (F3) 512, 64 ms with 16 transients.

The 3D ^{15}N-edited NOESY-HSQC (Marion *et al.*, 1989; Zuiderweg and Fesik, 1989) was recorded on a Bruker DMX750 spectrometer with the following numbers of complex points and acquisition times: ^{1}H (F1) 128, 13 ms, ^{15}N (F2) 21, 8.4 ms, ^{1}H (F3) 1024, 100 ms with 16 transients. The mixing time was 100 ms.

The 3D ^{13}C-edited NOESY-HSQC (Muhandiram, 1993) was recorded with the following numbers of complex points and acquisition times: ^{1}H (F1) 128, 26 ms, ^{13}C (F2) 32, 8.9 ms, ^{1}H (F3) 416, 52 ms with 16 transients. The 3D simultaneous ^{13}C/^{15}N-edited NOESY-HMQC (Pascal *et al.*, 1994) was recorded on a UNITY-plus 500 spectrometer with the following numbers of complex points and acquisition times: ^{1}H (F1) 128, 26 ms, ^{13}C (F2) 32, 12 ms, ^{1}H (F3) 416, 52 ms with 16 transients. The mixing times were 100 ms and 150 ms for ^{13}C-edited NOESY-HMQC and simultaneous ^{13}C/^{15}N-edited NOESY-HMQC experiments, respectively.

Two-dimensional (2D) ^{13}C-filtered TOCSY and [^{13}C/F1]-edited [^{13}C/F3]-filtered NOESY (Lee *et al.*, 1994) spectra was recorded on a UNITY 500 spectrometer with the following number of complex points and acquisition times: ^{1}H (F1) 256, 51 ms, ^{1}H (F2) 512, 73 ms (64 transients) for TOCSY, and ^{1}H (F1) 127, 29 ms, ^{1}H (F2) 416, 59 ms (256 transients) for NOESY.

II-2-3. Structural constraints

NOEs were assigned from 2D homonuclear and 3D heteronuclear NOESY spectra. The upper distance bounds obtained from the all NOESY spectra were grouped into four classes: 2.9, 3.5, 5.0, and 6.0 Å, respectively, corresponding to strong, medium, weak, and very weak NOEs. The lower bounds for the interproton distance restraints were set to the sum of the van der Waals radii of two protons. Upper distance limits for distance involving methyl protons and non-stereospecifically assigned methylene protons were corrected appropriately for center averaging (Wüthrich *et al.*, 1983), and additional 0.5 Å was added to the upper distance limits for NOEs involving methyl protons (Clore *et al.*, 1987; Wagner *et al.*, 1987). Phi and psi dihedral angle restraints were derived

from $^3J_{NH\alpha}$ coupling constants measured from $^1H/^{15}N$ HMQC-J spectrum and chemical shift indices (Wishart and Sykes, 1994). Values of -60° ± 30° and -40° ± 30° were used for phi and psi dihedral angles, respectively, in α-helical regions; -120° ± 30° and 120° ± 60° in β-strands. Hydrogen bond restraints were obtained by analyzing the $^1H/^2H$ exchange rates and the NOE patterns characteristic of α-helices or β-strands. Two distance restraints, r_{NH-O} (1.8-2.3 Å) and r_{N-O} (2.3-3.3 Å), were used for each hydrogen bond.

II-2-4. Structure calculation

Structure calculations were performed using a restrained molecular dynamics simulated annealing protocol within X-PLOR 3.1 (Brünger, 1993). Structure calculations employed 1786 interproton distance restraints (comprising 556 intraresidue, 440 sequential, 260 short-range, 507 long-range, 13 protein-ATP analogue, and 10 intra-analogue) obtained from heteronuclear three-dimensional nuclear Overhauser effect (NOE) spectra. In addition to the NOE-derived distance restraints, 92 distance restraints for 46 hydrogen bonds and 122 dihedral angle restraints were included in the structure calculation.

II-2-5. Sequence alignment

Sequence alignment of catalytic domains of histidine kinase family members are obtained from ψ-BLAST search (Altschul *et al.*, 1997) and MEGALIGN (DNASTAR Inc.). Among the SWISS-PROT database, approximately 150 homologous sequences are identified with an expectation (E) value of 0.01 by ψ-BLAST algorithm. The accession numbers of the SWISS-PROT database for the 10 selected sequences are P02933 (EnvZ), P08336 (CpxA), P08400 (PhoR), P23837 (PhoQ), P30844 (BasS), P21865 (KdpD), P14377 (HydH), P22763 (ArcB), P14376 (RcsC), and P10728 (SpoIIAB).

II-3. RESULTS

II-3-1. Resonance assignments

Previously described methodology for higher molecular weight (15 kDa and above) proteins (Ikura *et al.*, 1990; Powers *et al.*, 1992) were used to assign the backbone resonances in $^{13}C/^{15}N$ labeled EnvZ domain B. Heteronuclear 3D experiments correlating various intra-residue (i) and sequential (i-1) resonances were run in pairs. Sequential links between amino acid spin systems were initially established based on a pairwise comparison of NH inter- and intra-residual C^{α}, C^{β}, C^{o}, H^{α}, and H^{β} chemical shifts. When the intraresidual and sequential chemical shifts align, then the NHs are defined as sequential. A contiguous series of amide protons are examined for shift information about their amino acid type. A series is subsequently fit into the amino acid sequence of domain B. More than ninety percent of ^{1}H, ^{13}C, and ^{15}N backbone resonance assignments were obtained for non-proline residues.

Side-chain assignments were mainly assigned by their correlation to $^{13}C_{\alpha}$-$^{1}H_{\alpha}$ and $^{13}C_{\beta}$-$^{1}H_{\beta}$ crosspeaks in a HCCH-TOCSY spectrum. The carbon chemical shifts were obtained also by the ^{13}C-edited NOESY-HMQC spectrum. Backbone and side-chain ^{1}H, ^{13}C, and ^{15}N chemical shifts are reported in Table II-1.

II-3-2. Secondary structure

In order to determine the secondary structure of domain B, the chemical shift index (CSI) (Wishart *et al.*, 1995) was calculated using the C^{α} and C^{β} chemical shifts of domain B. The CSI relies on the observation that C^{α} and C^{β} chemical shifts for a given amino acid type tend to cluster in certain spectral regions depending on the secondary structure context (Venters *et al.*, 1996). The analysis (Figure II-2) reveals four helices (positive CSI) and seven strands (negative CSI). Sequential and short-range ($|i - j| < 5$) NOEs, $^{3}J_{NH\alpha}$ coupling constants and slowly exchanging backbone amide protons are summarized in Figure II-3. The positions and length of the helices match closely with small $^{3}J_{NH\alpha}$ coupling constants, slow NH exchange rates, and the NOE analysis: strong $d_{NN}(i, i+1)$ and $d_{\alpha N}(i, i+3)$ NOE connectivities.

II-3-3. Structure description

The solution structure of domain B was determined on the basis of 1786 interproton distance restraints (comprising 556 intra residue, 440 sequential, 260 short-range, 507 long-range, 13 protein-ATP analogue, and 10 intra-analogue) obtained from heteronuclear 3D NOE spectra. Intermolecular NOEs between domain B and AMP-PNP were identified from [^{13}C/F1]-edited [^{13}C/F3]-filtered HMQC-NOESY spectrum. In addition to the NOE-derived distance restraints, 92 distance restraints for 46 hydrogen bonds and 122 dihedral angle restraints were included in the structure calculation. Figure II-4a shows a best-fit superposition of the determined structure of domain B. The structure reveals an α/β sandwich fold: one layer consists of a five-stranded β-sheet (strand B, residues 319-323; D, 356-362; E, 367-373; F, 420-423; G, 431-436), and the other layer comprises three α helices (α1, 301–311; α2, 334–343; α4, 410–414) (Figure II-4b). Two adjacent parallel β strands, B and F connected by helix α2, display an unusual "left-handed" connectivity (Branden and Tooze, 1991). The structure is well defined with a root-mean-square (rms) deviation between backbone atom coordinates of 0.57 ± 0.12 Å, and 0.94 ± 0.08 Å for all heavy atoms of residues in the β-sheets and α-helices. The average rmsd values from idealized geometry for bonds, angles and impropers are 0.005 Å, 0.61° and 0.39°, respectively. The total and Lennard-Jones potential energies are 516 ± 70 and -134 ± 29 kcal mol^{-1}, respectively. None of the structures has violations greater than 0.40 Å for distance restraints and 3.0 Å for dihedral angle restraints.

II-4. DISCUSSION

The two α/β layers enclose an extensive hydrophobic core, augmented by a small anti-parallel β-sheet (strand A, 297-299; C, 330-332) that seals the sandwich at one end. These structurally critical hydrophobic residues are highly conserved over homologous histidine kinase domains, as would be expected (Figure II-5). It also reveals a characteristic fold of a long polypeptide segment that extends away from the rest of the molecule (Figure II-4b). This segment consists of a short α-

helix, α3 (residues 380-384), followed by a long loop (residues 385-409), which referred as the central loop. Almost no short- or long-range NOEs were detected for the residues in this loop, and the chemical shifts and $^3J_{NH\alpha}$ were nearly the same as those in a random coil (Figure II-3). Moreover, ^1H-^{15}N heteronuclear NOE measurements showed smaller NOE values (0.49 ± 0.10) for the residues in this loop than the values (0.75 ± 0.12) of the structurally well-defined region, suggesting that the region is mobile in solution. The lack of domain A for the truncated domain B sample may cause this high mobility of the central loop.

Like eukaryotic protein kinases, histidine kinases requires the presence of ATP and Mg^{2+} for their activity. The present structure contains a nonhydrolysable ATP (AMP-PNP) whose location in the structure has been determined on the basis of a 13 intermolecular NOEs observed between Ile-378/Leu-386/Leu-422 side-chain protons and the adenosine H2, H8, H1' and H5' protons. The AMP-PNP molecule is surrounded by helix α3 and part of the central loop, and makes additional contacts with strands F and G. The AMP-PNP adenine ring is in close spatial proximity to Asn-347, Asp-373, Ile-378, Leu-386, and Phe-387 (Figure II-4b), which are conserved in members of the histidine kinase family (Figure II-5). The triphosphate chain is exposed to the protein surface, consistent with the potential to transfer the γ-phosphate to His-243 in domain A. Moreover, five glycines (Gly-375, -377, -403, -405, -429) and an asparagine (Asn-347) in the catalytic core are highly conserved and strategically located in the structure (Figure II-4b), indicating their structural and functional significance. Previous mutagenesis studies (Yang and Inouye, 1993) demonstrated that the glycine-rich regions, G1 and G2 boxes, are essential for kinase activity. Further, the present structure in this study shows that Gly-375 and Gly-429 are particularly important, allowing sharp kinks forming between strand E and helix α3 and between strands F and G, respectively, that contour part of the AMP-PNP binding site.

High deviations in the central loop in the NMR-derived structure of domain B, due to high mobility, precludes close examination of the residues that could be involved in the catalysis. However, further information can be obtained from a variety of database searches and structural comparisons. There found similar fold (βαβ left handed connectivity) in the ATP binding regions of Hsp90 and DNA gyrase B subunit (Figure II-6). Both ATP binding domains of Hsp90 and DNA

gyrase B subunit were already known to have similar folds. Besides all three proteins requiring ATP binding to their function, what are common to them are helix α2, four strands (D, E, F, and G), and the central loop. They also enclose Asn-347 and the glycine-rich sequence motifs (G1, DxGxGϕ; G2, GϕGϕ; ϕ=hydrophobic residues), both occur in all three families and are close to the ATP binding site of Hsp90.

In detail, the Hsp90-ADP complex shows its Asn-37 (corresponding to Asn-347 in EnvZ) binding directly to β phosphate and Mg^{2+} as well as indirectly to the adenine base. Interestingly, the EnvZ mutant N347D results in a phenotype in which ATP-dependent autokinase activity is lost, but phosphatase activity between the mutant protein and phosphorylated OmpR is retained (Dutta and Inouye, 1996). It also confirmed that ATP binding to EnvZ (223-450) is abolished in the N347D mutant (Tanaka *et al.*, 1998). The decreased ATP affinity of N347D provides compelling evidence that this conserved asparagine plays a critical role in ATP-dependent autophosphorylation activity of EnvZ.

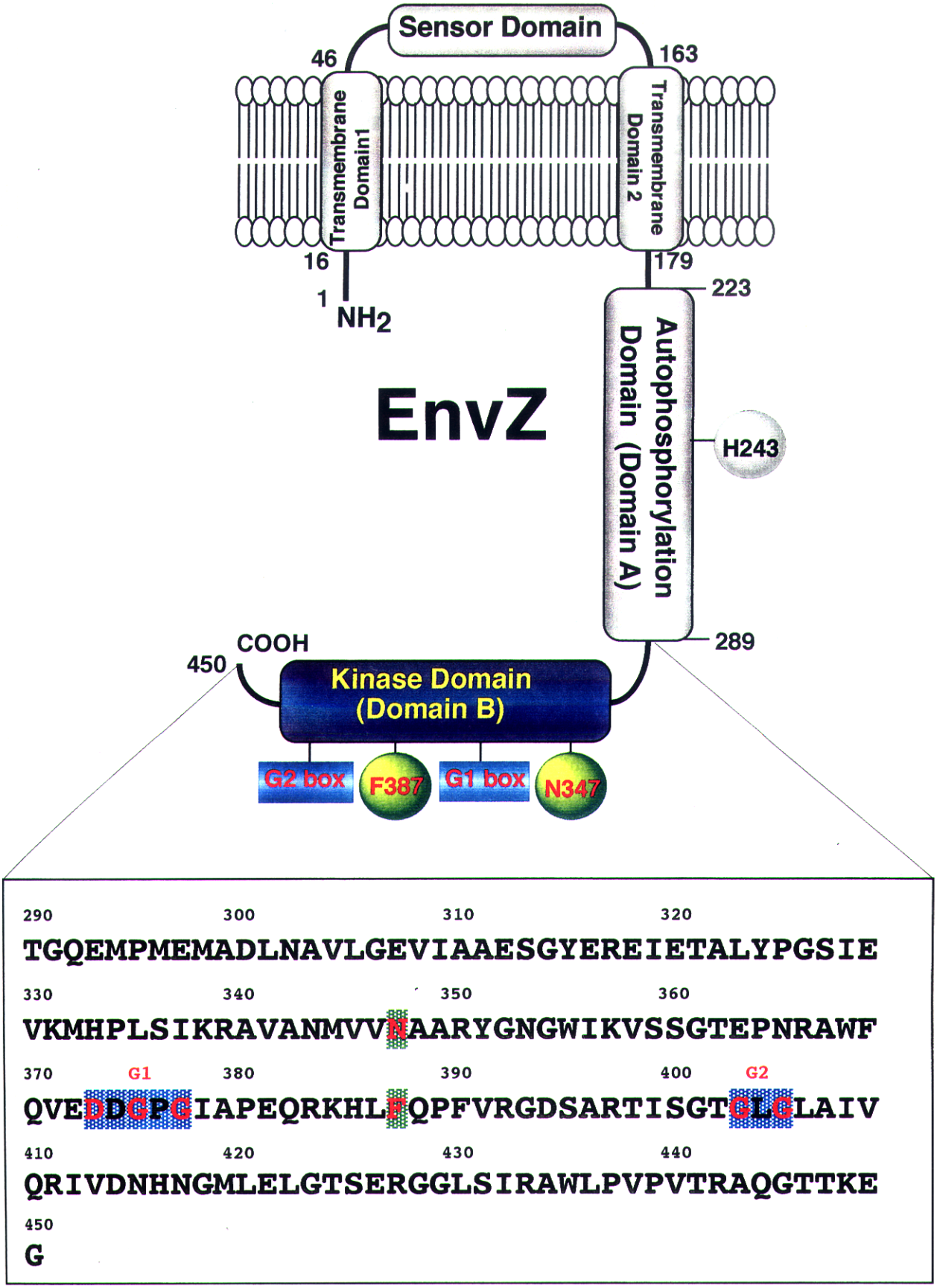

Figure II-1. Schematic presentation of the primary structure of domain B (highlighted in blue).

The conserved amino acid residues are labeled in red.

Table II-1.

^{15}N, ^{13}C, ^{13}CO, and ^{1}H Resonance Assignments for EnvZ Domain B at pH 7.0 and 25 ° C[a]

residue	N	CO	C^{α}	C^{β}	others
T290	-	176.3	62.1 (3.67)	70.0 (4.15)	$C^{\gamma 2}$ 20.7 (1.29)
G291	111.6 (8.70)	173.5	45.2		
Q292	119.9 (8.39)	175.5	55.6 (4.34)	29.3 (1.95, 2.11)	C^{γ} 33.5 (2.35)
E293	121.9 (8.53)	175.8	56.6 (4.21)	30.0 (1.95)	C^{γ} 36.1 (2.23)
M294	121.6 (8.35)	172.6	52.6 (4.31)	32.6 (1.63, 1.73)	C^{γ} 31.7 (2.34)
P295		176.5	63.0 (4.40)	31.6 (2.00, 2.20)	C^{γ} 27.3 (1.98, 2.20); C^{δ} 50.0 (3.38, 3.58)
M296	120.5 (8.31)	175.3	54.8 (4.65)	34.9 (1.58, 1.98)	C^{γ} 32.6 (2.19, 2.60); C^{ε} 17.5 (1.60)
E297	120.2 (9.21)	174.0	54.0 (4.80)	33.7 (2.10)	C^{γ} - (2.36)
M298	119.6 (8.63)	175.9	54.3 (4.97)	30.9 (2.00)	C^{γ} 31.7 (2.60); C^{ε} 16.3 (1.98)
A299	128.4 (9.05)	174.2	51.0 (4.69)	22.5 (1.37)	
D300	117.6 (8.39)	177.4	52.2 (4.89)	41.1 (2.74, 2.88)	
L301	128.9 (9.53)	177.6	57.7 (3.78)	43.4	C^{γ} 26.5 (1.47); $C^{\delta 1}$ 25.5 (0.86); $C^{\delta 2}$ 22.3 (0.66)
N302	113.7 (8.24)	178.8	55.0 (4.59)	37.5 (2.67, 3.22)	N^{δ} 111.5 (6.55, 7.61)
A303	125.6 (7.37)	180.0	54.7 (4.17)	17.8 (1.59)	
V304	119.0 (7.34)	177.6	66.2 (3.65)	31.6 (1.98)	$C^{\gamma 1}$ 21.2 (0.73); $C^{\gamma 2}$ 22.0 (1.01)
L305	116.9 (8.18)	178.9	58.0 (3.71)	41.5 (1.07, 1.92)	C^{γ} 26.3 (1.75); $C^{\delta 1}$ 26.7 (0.80); $C^{\delta 2}$ 23.0 (0.31)
G306	104.1 (8.16)	176.0	46.9 (3.67, 3.93)		
E307	121.2 (7.69)	179.2	59.4 (4.07)	29.7 (2.03, 2.21)	C^{γ} 36.4 (2.54)
V308	119.9 (7.60)	177.2	65.9 (3.81)	31.6 (2.03)	$C^{\gamma 1}$ 20.6 (0.91); $C^{\gamma 2}$ 22.5 (1.13)
I309	119.4 (8.46)	177.9	65.5 (3.35)	38.0 (1.80)	$C^{\gamma 1}$ - (1.63, 1.75); $C^{\gamma 2}$ 17.2 (0.82); $C^{\delta 1}$ 13.6 (0.74)
A310	120.3 (7.88)	179.3	54.6 (4.13)	17.9 (1.47)	
A311	119.4 (7.53)	179.2	54.0 (4.22)	19.0 (1.57)	
E312	115.1 (8.08)	176.4	55.6 (4.44)	29.4 (1.62, 2.21)	C^{γ} 35.2 (2.00, 2.43)

S313	115.1 (7.68)	174.2	59.1 (4.59)	64.0 (3.92, 4.01)	
G314	109.3 (8.23)	176.2	45.3 (3.96)		
Y315	119.9 (8.20)	175.9	58.5 (4.50)	37.8 (2.99, 3.13)	C^{δ} 132.6 (7.13); C^{ε} 117.9 (6.84)
E316	117.7 (8.57)	175.5	57.3 (4.12)	28.8 (2.13)	
R317	118.7 (7.72)	174.3	55.1 (4.55)	31.5 (1.74)	C^{γ} 26.8 (1.56); C^{δ} 43.2 (3.08, 3.19)
E318	123.8 (8.57)	175.7	55.7 (4.49)	30.6 (1.98, 2.10)	C^{γ} - (2.28)
I319	124.5 (8.40)	175.3	60.7 (4.25)	39.7 (1.61)	$C^{\gamma 1}$ 27.9 (1.53); $C^{\gamma 2}$ 16.9 (0.65); $C^{\delta 1}$ 13.3 (0.73)
E320	129.9 (8.96)	175.2	55.9 (4.50)	30.3 (1.91, 2.06)	C^{γ} 36.5 (2.15, 2.52)
T321	115.4 (8.72)	174.0	59.7 (5.28)	71.2 (4.07)	$C^{\gamma 2}$ 21.8 (1.16)
A322	129.4 (8.65)	176.0	51.0 (4.71)	18.9 (1.38)	
L323	122.6 (8.65)	177.0	54.0 (4.45)	39.9 (1.24, 1.59)	$C^{\delta 1}$ 21.8 (0.63); $C^{\delta 2}$ 24.9 (0.75)
Y324	127.6 (8.13)	-	55.9 (4.52)	40.0 (2.43, 3.08)	C^{δ} 133.3 (7.06); C^{ε} 117.9 (6.82)
P325		175.0	62.6 (4.31)	29.8 (1.88)	C^{γ} 27.0 (1.55, 1.78); C^{δ} 50.2 (2.58, 3.50)
G326	110.7 (7.81)	172.1	44.7 (3.97)		
S327	115.7 (8.38)	174.4	57.7 (4.92)	64.8 (3.70)	
I328	124.3 (8.54)	173.8	60.6 (4.14)	40.5 (1.61)	$C^{\gamma 1}$ 26.5 (1.48); $C^{\gamma 2}$ 17.6 (0.70); $C^{\delta 1}$ 13.5 (0.50)
E329	127.3 (8.45)	175.6	56.8 (4.80)	29.7 (1.87)	C^{γ} 36.8 (1.97, 2.13)
V330	120.1 (8.89)	173.3	59.5 (4.53)	36.2 (2.20)	$C^{\gamma 1}$ 22.5 (1.03); $C^{\gamma 2}$ 20.9 (0.92)
K331	124.7 (8.70)	175.4	55.7 (4.78)	32.5 (1.68, 1.82)	C^{γ} 25.6 (1.28); C^{δ} 29.1 (1.66); C^{ε} 41.9 (2.92)
M332	120.1 (9.43)	174.0	55.4 (5.52)	36.4 (2.04)	C^{ε} 17.8 (1.85)
H333	125.2 (11.08)	174.6	53.6 (5.63)	31.5 (3.10, 3.36)	$C^{\delta 2}$ 118.2 (7.55); $C^{\varepsilon 1}$ 137.5 (7.83)
P334		177.5	66.6 (4.03)	32.2 (1.94, 2.20)	C^{δ} 51.1 (3.89, 4.50)
L335	114.7 (7.85)	179.4	58.2 (3.89)	41.2 (1.35, 1.55)	C^{γ} 27.0 (1.64); C^{δ} 24.0 (0.93), 24.2 (0.97)
S336	115.4 (7.41)	175.6	62.0 (4.37)	- (4.14)	
I337	123.0 (7.89)	177.5	61.6 (3.72)	33.7 (2.10)	$C^{\gamma 2}$ 16.4 (0.43); $C^{\delta 1}$ 5.4 (0.00)
K338	118.4 (8.59)	177.7	61.0 (3.51)	31.9 (1.73, 1.84)	C^{γ} 26.8 (1.11, 1.56); C^{δ} 29.4 (1.66);

					C^{ε} 41.6 (2.72, 2.75)
R339	118.8 (7.59)	177.9	58.7 (4.03)	29.8	C^{δ} 43.1 (3.24)
A340	121.0 (8.31)	178.4	55.0 (4.11)	17.2 (1.67)	
V341	116.3 (8.57)	178.1	65.9 (3.75)	31.5 (1.98)	$C^{\gamma 1}$ 20.9 (0.78); $C^{\gamma 2}$ 22.7 (0.57)
A342	122.8 (8.80)	178.8	55.9 (3.80)	17.6 (1.53)	
N343	116.1 (8.33)	179.0	56.4 (4.28)	37.4 (3.04)	
M344	118.7 (7.93)	-	56.5 (4.05)		C^{ε} 18.0 (1.95)
V345	-	176.5	67.2 (3.52)	31.3	C^{γ} 21.5 (0.83), 23.3 (0.87)
V346	119.2 (9.00)	-	66.6 (3.67)	31.2 (2.06)	C^{γ} 20.9 (0.95), 22.7 (1.05)
N347	-	176.0	53.7 (4.68)	38.6 (2.79, 2.85)	
A348	123.6 (7.93)	180.3	54.6 (4.33)	19.1 (1.66)	
A349	120.5 (8.31)	178.2	54.0 (3.99)	18.2 (1.37)	
R350	117.1 (8.11)	177.7	57.9 (3.88)	30.6	C^{γ} 26.4 (1.20, 1.93); C^{δ} 43.0 (2.78, 2.87)
Y351	114.4 (8.25)	176.5	61.4 (4.50)	37.5	
G352	105.3 (7.14)	-	43.6		
N353	-	175.2	53.0 (5.19)	40.2 (2.64, 3.09)	N^{δ} 114.8 (7.12, 7.64)
G354	110.0 (8.95)	173.7	45.4 (3.65)		
W355	124.2 (8.68)	175.7	57.9 (5.04)	29.1 (2.92, 3.05)	$C^{\delta 1}$ - (7.31); $N^{\varepsilon 1}$ 131.6 (10.35)
I356	128.2 (7.86)	172.6	60.0 (4.52)	42.3 (1.57)	$C^{\gamma 2}$ 16.8 (0.70)
K357	124.8 (7.90)	176.1	53.2 (5.30)	36.9	
V358	129.6 (8.74)	173.3	60.3 (5.33)	33.7 (1.75)	$C^{\gamma 1}$ 20.7 (0.94); $C^{\gamma 2}$ 21.2 (0.84)
S359	119.4 (9.21)	171.6	56.4 (4.82)	67.3 (3.97, 4.12)	
S360	112.1 (7.57)	171.2	55.4 (4.48)	66.8	
G361	102.9 (6.74)	169.2	44.8 (3.66)		
T362	107.5 (7.81)	171.6	60.1 (4.92)	71.1 (3.79)	$C^{\gamma 2}$ 19.4 (0.58)
E363	124.7 (9.04)	174.3	54.3 (4.95)	31.0	C^{γ} 36.3 (2.59)
P364		176.2	66.1 (4.31)	31.2 (1.87, 2.37)	C^{γ} 28.0 (2.04, 2.25); C^{δ} 50.2 (3.78, 3.91)
N365	110.8 (8.56)	175.5	54.1 (4.84)	39.1 (3.01, 3.08)	N^{δ} 112.6 (6.94, 7.58)
R366	118.7 (7.97)	172.3	56.3 (5.35)	34.9 (1.95, 2.27)	C^{γ} 25.9 (1.73, 1.75)

A367	124.5 (9.54)	174.9	50.2 (5.14)	23.3 (1.34)	
W368	114.4 (8.26)	174.3	54.4 (5.81)	31.6	$C^{\delta 1}$ - (6.41); $C^{\varepsilon 3}$ - (6.37); $C^{\zeta 2}$ - (7.28); $C^{\zeta 3}$ - (6.72); $C^{\eta 2}$ - (6.88); $N^{\varepsilon 1}$ 128.8 (10.26)
F369	110.4 (8.33)	172.8	55.8 (5.46)	43.3 (2.92, 3.06)	C^{δ} 132.2 (6.98); C^{ε} 130.2 (7.08); C^{ζ} 128.0 (6.73)
Q370	122.3 (9.20)	173.0	54.4 (5.76)	29.8	
V371	124.1 (8.81)	174.1	61.4 (4.99)	34.5 (1.96)	$C^{\gamma 1}$ 21.2 (0.88); $C^{\gamma 2}$ 22.1 (1.12)
E372	126.4 (8.91)	174.0	54.2 (5.75)	37.3	
D373	113.5 (7.88)	175.6	53.6 (5.87)	46.4 (2.85, 3.28)	
D374	118.6 (9.00)	177.1	52.1 (4.87)	41.4 (2.78, 3.31)	
G375	108.2 (9.99)	-	45.5		
P376		178.5	63.1	32.4	
G377	111.6 (9.67)	171.6	43.9 (3.50, 4.23)		
I378	115.8 (7.82)	174.9	60.4 (4.12)	39.6 (1.20)	$C^{\gamma 1}$ 26.6 (0.39); $C^{\gamma 2}$ 17.3 (0.70); $C^{\delta 1}$ 12.6 (-0.09)
A379	132.5 (8.85)	176.4	51.2 (4.52)	17.3 (1.52)	
P380		178.7	66.4 (3.88)	32.0 (1.98, 2.36)	C^{γ} - (2.26); C^{δ} 50.1 (3.83, 3.91)
E381	116.2 (9.35)	177.6	59.2 (4.08)	28.5 (2.05)	C^{γ} 36.0 (2.35)
Q382	116.9 (7.54)	177.7	56.9 (4.35)	28.7 (2.11)	C^{γ} 33.8 (2.37, 2.43)
K384	115.4 (7.53)	177.3	58.2 (4.07)	32.0 (1.68, 1.71)	C^{γ} 24.0 (1.21, 1.23); C^{δ} 28.8 (1.64); C^{ε} 41.4 (2.93)
H385	115.3 (7.48)	175.3	55.7 (4.68)	29.6 (3.00, 3.24)	$C^{\delta 2}$ 119.9 (7.02); $C^{\varepsilon 1}$ - (7.87)
I386	118.8 (7.37)	176.4	56.3 (3.99)	42.8 (1.33)	C^{γ} 26.2 (1.45); C^{δ} 23.2 (0.64), 25.0 (0.68)
F387	114.1 (7.82)	175.0	56.8 (4.60)	38.5 (2.92, 3.30)	C^{δ} 131.7 (7.24); C^{ε} 130.4 (7.16); C^{ζ} 128.2 (7.01)
Q388	120.4 (7.93)	173.6	53.7 (4.64)	28.9 (1.99, 2.13)	C^{γ} 33.3 (2.41)
P389		177.4	63.2 (4.42)	31.9 (1.81, 2.21)	C^{γ} 27.3 (1.99); C^{δ} 50.2 (3.65, 3.76)
F390	119.5 (8.21)	175.2	57.5 (4.66)	39.4 (3.09, 3.14)	C^{δ} - (7.24)

V391	122.4 (8.07)	175.3	62.0 (4.07)	32.9 (2.03)	C^{γ} 20.6 (0.91)
R392	124.5 (8.37)	176.5	56.2 (4.26)	30.5 (1.80, 1.88)	C^{γ} 27.0 (1.64, 1.71); C^{δ} 42.9 (3.23)
G393	110.3 (8.50)	173.7	45.3		
D394	120.3 (8.25)	176.4	54.2 (4.66)	41.2 (2.69, 2.74)	
S395	116.0 (8.31)	174.2	58.8 (4.39)	63.5 (3.92, 4.01)	
A396	124.6 (8.33)	177.4	52.7	19.0 (1.44)	
R397	118.5 (8.08)	176.1	56.1 (4.38)	30.8	
T398	114.4 (8.13)	174.4	61.8	69.7	
I399	122.0 (8.17)	175.8	61.6 (4.23)	38.7 (1.90)	$C^{\gamma 1}$ 27.1 (1.19, 1.50); $C^{\gamma 2}$ 17.3 (0.92); $C^{\delta 1}$ 12.9 (0.85)
S400	118.5 (8.31)	174.6	58.3 (4.49)	63.9 (3.88, 3.90)	
G401	110.6 (8.42)	173.9	45.4		
T402	112.2 (8.08)	174.5	61.7	70.0	
G403	110.8 (8.53)	-	45.6		
L404	-	-	-		
G405	-	-	-		
L406	-	176.5	54.4	41.3	
A407	120.6 (8.33)	-	54.2	18.3	
I408	-	-	64.2 (3.82)	37.4 (2.05)	$C^{\gamma 1}$ 29.0 (1.25, 1.69); $C^{\gamma 2}$ - (0.93); $C^{\delta 1}$ 12.8 (0.87)
V409	-	-	67.4 (3.45)	-	C^{γ} 22.5 (1.01), - (0.92)
Q410	-	177.2	59.3 (3.78)	28.7 (2.17)	C^{γ} 33.5 (2.28); N^{ε} 111.2 (6.64, 7.34)
R411	118.9 (7.91)	178.4	59.0 (4.17)	29.8	C^{γ} 26.8 (1.79); C^{δ} 43.1 (3.25)
I412	120.0 (8.42)	179.5	65.7 (3.92)	38.9 (2.05)	$C^{\gamma 1}$ - (1.40); $C^{\gamma 2}$ 17.2 (0.93); $C^{\delta 1}$ 14.4 (1.05)
V413	122.5 (8.91)	178.7	68.3 (3.45)	30.6 (2.16)	$C^{\gamma 1}$ 21.3 (0.81); $C^{\gamma 2}$ 23.3 (0.91)
D414	123.6 (9.02)	180.5	58.1 (4.56)	40.5 (2.78, 2.97)	
N415	119.5 (8.60)	175.5	55.2 (4.63)	38.4 (2.87, 3.21)	N^{δ} 110.0 (6.94, 7.60)
H416	115.7 (7.72)	173.4	58.0 (4.37)	29.2 (2.93, 3.80)	$C^{\delta 2}$ - (7.29); $C^{\varepsilon 1}$ 136.8 (7.80)

N417	114.7 (8.41)	174.2	54.5 (4.65)	36.9 (3.04, 3.21)	
G418	102.9 (8.19)	173.3	44.4 (4.15, 4.72)		
M419	116.6 (8.27)	173.1	54.9 (4.72)	36.3 (1.97, 2.06)	C^{γ} 31.5 (2.47); C^{ε} 17.0 (1.85)
L420	124.2 (8.93)	175.8	53.4 (5.44)	45.6 (1.37)	C^{γ} 27.1 (1.50); $C^{\delta 1}$ 24.4 (0.75); $C^{\delta 2}$ 25.0 (0.72)
E421	122.9 (9.50)	174.1	55.3 (4.72)	34.1	
L422	127.5 (8.92)	176.0	54.3 (5.16)	43.5 (1.43, 1.71)	C^{δ} 24.7 (0.82), 24.9 (0.82)
G423	110.3 (8.93)	173.2	45.1 (4.41)		
T424	121.5 (8.81)	174.2	61.3 (5.11)	70.6 (3.90)	$C^{\gamma 2}$ 21.2 (1.47)
S425	122.5 (9.03)	175.8	56.7 (4.72)	67.2 (3.99)	
E426	120.1 (9.01)	176.4	58.6 (4.22)	30.2 (2.12, 2.19)	C^{γ} 35.9 (2.39)
R427	113.0 (7.29)	175.6	55.0 (4.54)	30.2	C^{γ} 26.4 (0.22, 0.81); C^{δ} 42.5 (1.60, 2.53)
G428	107.7 (7.73)	173.3	46.2 (3.57, 4.30)		
G429	107.5 (7.31)	174.5	44.4 (3.69, 4.57)		
L430	124.3 (8.48)	177.1	55.7 (4.63)	42.6	C^{δ} 23.1 (0.89), 25.7 (0.64)
S431	119.7 (7.94)	172.7	55.8 (5.06)	64.5 (3.13, 3.18)	
I432	125.7 (8.87)	171.4	59.2 (4.94)	40.9	
R433	128.3 (8.82)	172.9	53.3 (5.02)	34.0	
A434	128.0 (8.50)	174.2	49.4 (5.03)	21.0 (0.29)	
W435	120.7 (9.05)	176.0	55.0 (5.51)	31.7 (3.11)	$C^{\delta 1}$ 126.5 (6.84); $C^{\varepsilon 3}$ - (7.47); $C^{\zeta 2}$ - (7.24); $C^{\zeta 3}$ - (6.79); $C^{\eta 2}$ - (6.93); $N^{\varepsilon 1}$ 130.8 (10.57)
L436	120.0 (9.58)	173.8	51.0 (5.18)	44.8 (1.53)	C^{γ} 27.1 (1.76); $C^{\delta 1}$ 25.8 (1.01); $C^{\delta 2}$ 23.1 (1.04)
P437		176.4	63.2 (4.80)	32.3 (2.05, 2.50)	C^{γ} 27.7 (2.25, 2.37); C^{δ} 50.7 (3.74, 3.98)
V438	118.3 (7.49)	173.9	59.0 (4.73)	32.9 (2.03)	C^{γ} 20.1 (0.91), 21.3 (1.06)
P439		176.3	62.9 (4.58)	32.0 (1.99, 2.35)	C^{γ} 27.3 (1.99, 2.10); C^{δ} 50.9 (3.86, 3.99)
V440	120.5 (8.28)	176.1	62.3 (4.22)	32.7 (2.13)	C^{γ} 20.5 (1.05), 20.8 (1.01)
T441	118.4 (8.29)	173.9	61.6 (4.40)	69.8 (4.22)	$C^{\gamma 2}$ 21.3 (1.19)

R442	123.9 (8.41)	175.5	55.7 (4.40)	30.9 (1.79, 1.90)	C^{γ} 26.8 (1.67); C^{δ} 42.9 (3.23)
A443	125.5 (8.42)	177.4	52.4 (4.34)	19.0 (1.42)	
Q444	119.8 (8.46)	176.2	55.9 (4.37)	29.5 (2.05, 2.16)	C^{γ} 33.5 (2.43)
G445	110.0 (8.51)	174.0	45.2		
T446	113.2 (8.16)	174.5	61.6 (4.47)	69.8 (4.29)	$C^{\gamma 2}$ 21.1 (1.24)
T447	116.5 (8.27)	174.0	61.6 (4.42)	69.8 (4.26)	$C^{\gamma 2}$ 21.1 (1.24)
K448	123.8 (8.43)	175.9	56.3 (4.37)	33.0 (1.80, 1.88)	C^{γ} 24.2 (1.45); C^{δ} 28.7 (1.71); C^{ε} 41.6 (3.02)
E449	122.6 (8.48)	175.5	56.4 (4.36)	30.4 (1.96, 2.11)	C^{γ} 36.0 (2.29)
G450	116.0 (8.02)	-	46.0		

[a] ^{15}N or ^{13}C chemical shift is given first, and the attached ^{1}H chemical shift(s) is in parenthesis. The chemical shift reference used for ^{1}H and ^{13}C is 3-(trimethylsilyl)propionate, sodium salt. ^{15}N chemical shift are reported relative to external liquid NH_3.

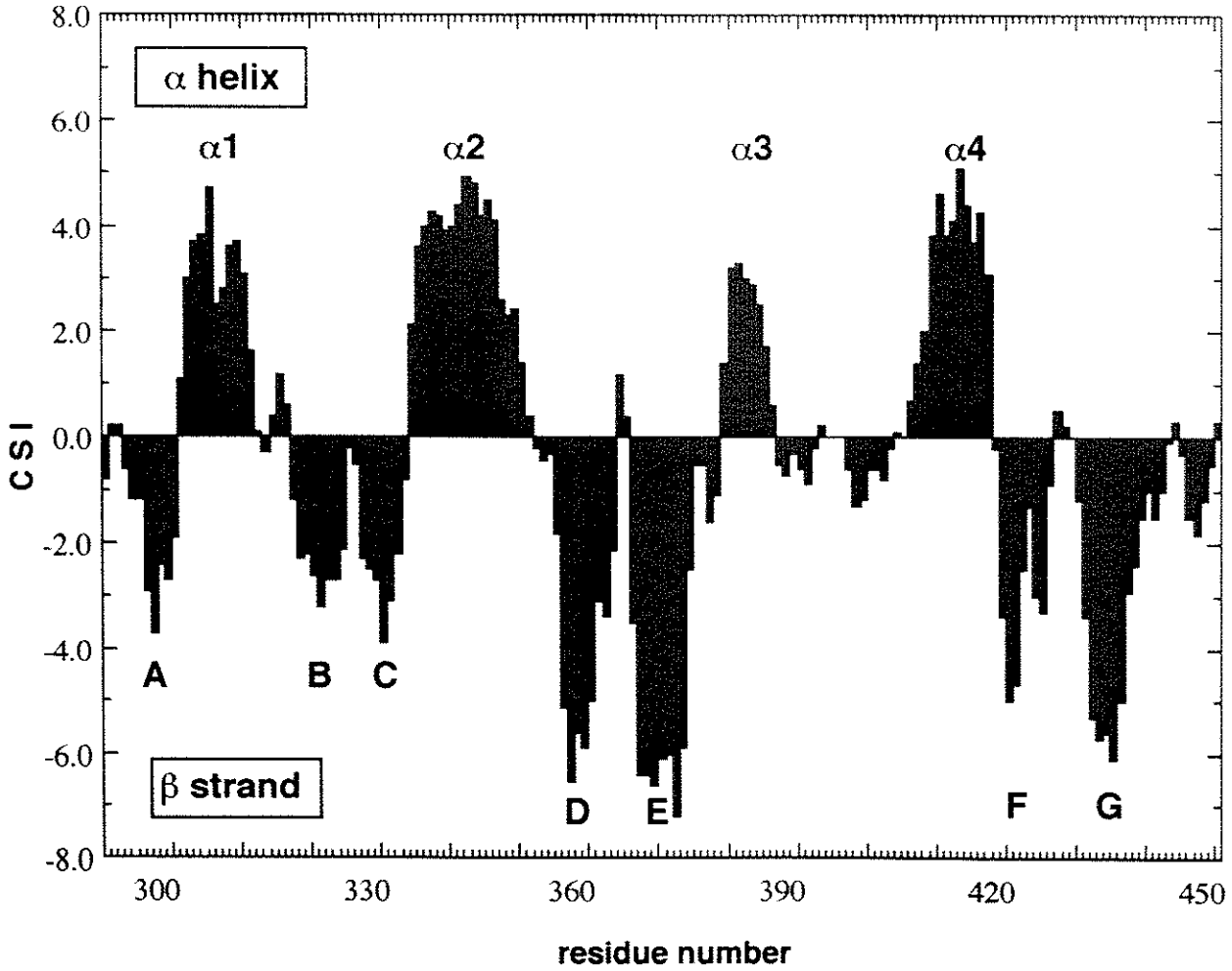

Figure II-2. Chemical shift index (CSI) of domain B (residues 290-450).

CSI versus amino acid sequence of domain B.
CSI = 0.25 * (1* dCαCβ[i-1]+2* dCαCβ[i]+1* dCαCβ[i+1])
dCαCβ[i] = dCα[i] - dCβ[i], dCα[i] = Cαrcoil - Cαobs [i], dCβ[i] = Cβrcoil - Cβobs[i]
(rcoil: random-coil chemical shift value, obs: observed chemical shift value)

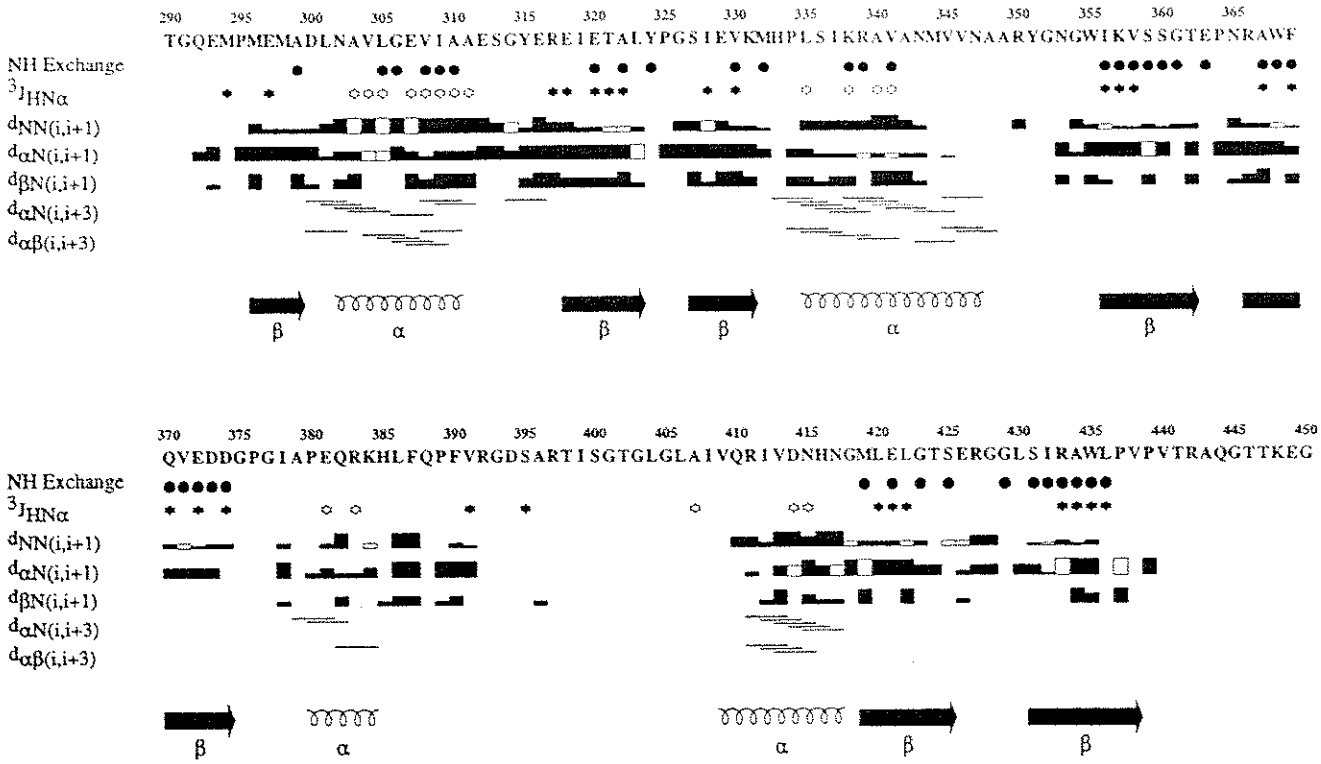

Figure II-3. Summary of sequential and medium-range NOEs involving NH, Hα, and Hβ resonances, amide hydrogen exchange data, and $^3J_{HN\alpha}$ coupling observed for domain B.

Backbone amide hydrogens that exchange slowly are indicated with filled circles. For the ^3JHNa data, large couplings (> 8 Hz) are denoted as filled stars and small couplings (< 5 Hz) as open stars. NOE connectivities [dNN(i, i+1), dαN(i, i+1), and dβN(i, i+1)] are represented as strong, medium, weak, or very weak intensity in bar graphs. NOEs that are uncertain because of spectral overlap are indicated by unfilled bars. At the bottom, cartoon representation of the secondary structure is shown.

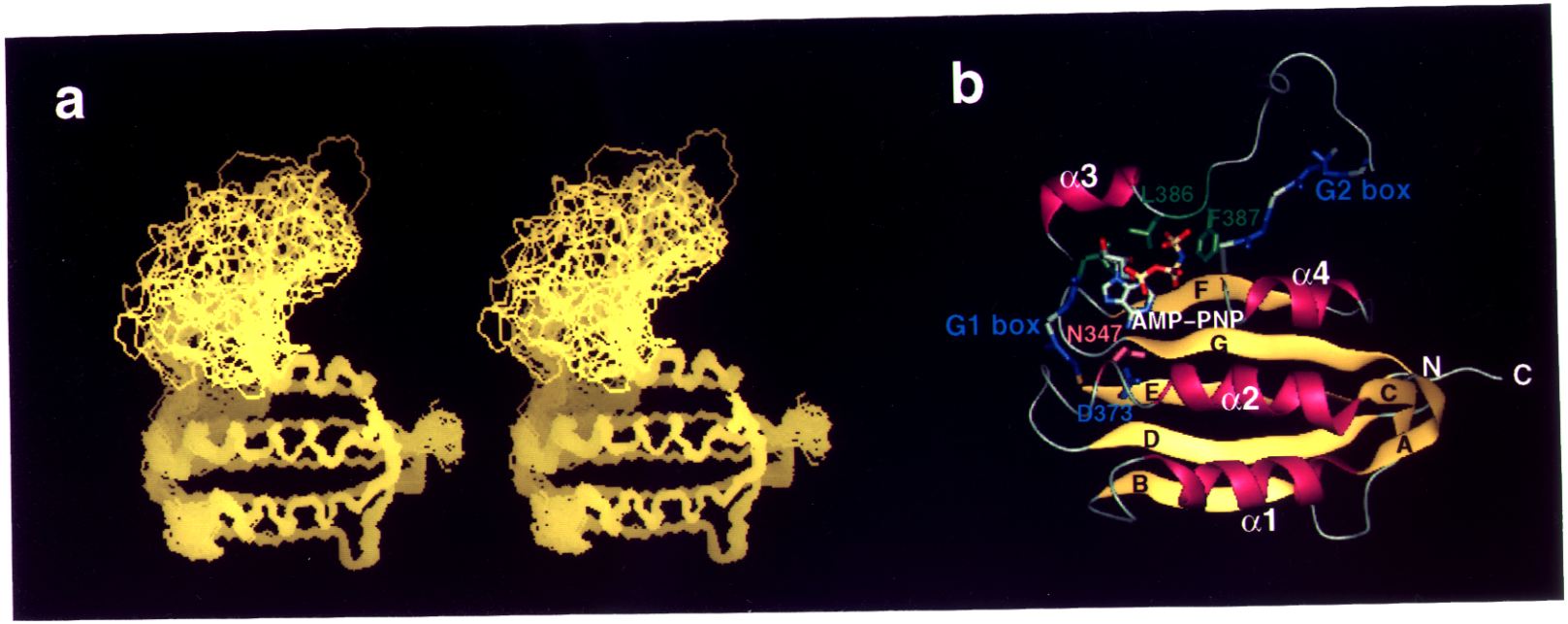

Figure II-4a. Stereoview of a best fit superposition of the backbone atoms (N, Cα, and C') of the 25 NMR-derived structures of domain B.

The main-chain atoms of the 25 structures are superimposed against the energy-minimized average structure using residues 297-299, 301-311, 319-323, 330-332, 334-343, 356-362, 367-373, 420-423 and 431-436. The N-terminal 5 and C-terminal 10 residues, which are also not well-defined due to the lack of a large number of experimental distance and dihedral angle restraints, are omitted in the figure. This figure was generated using Insight II (Molecular Simulations Inc., San Diego, CA).

II-4b. Schematic ribbon drawing of the energy-minimized average structure of domain B.

The ATP analogue (AMP-PNP) is shown as a stick model, and the helices (in magenta) and strands (in yellow) are labeled. The backbone heavy atoms of glycines in G1 and G2 boxes (in blue), and the side-chain heavy atoms of Asn-347 (in pink), Asp-373 (in blue), Ile-378, Leu-386, and Phe-387 (in green) are also shown as a stick model. The model was generated using Quanta (Molecular Simulations Inc., San Diego, CA).

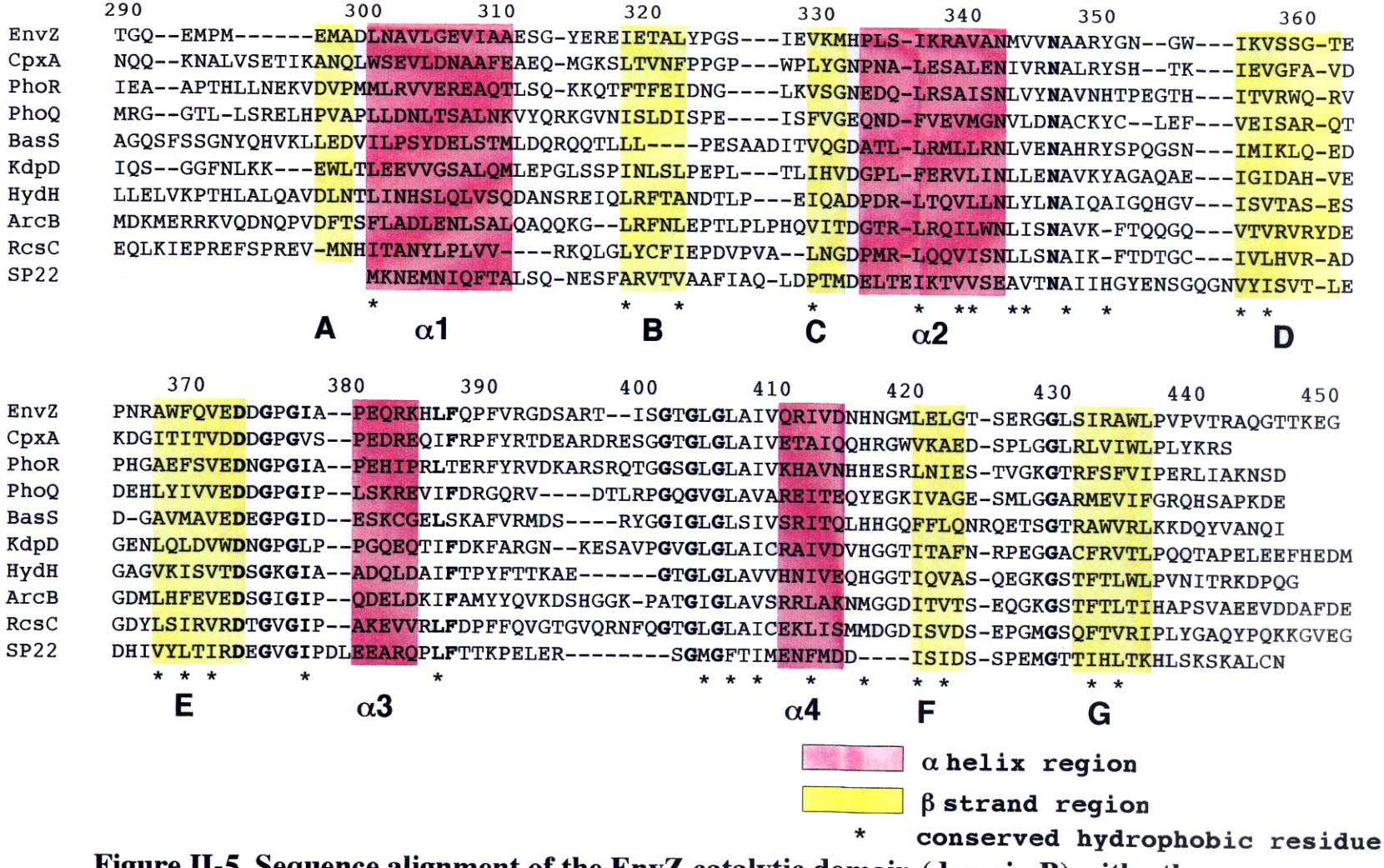

Figure II-5. Sequence alignment of the EnvZ catalytic domain (domain B) with other members of the histidine kinase family.

Secondary structural elements are shown by boxes colored as in Figure II-4b, with their notation indicated below the boxes. The residues that are found to be important in the ATP binding are shown in bold.

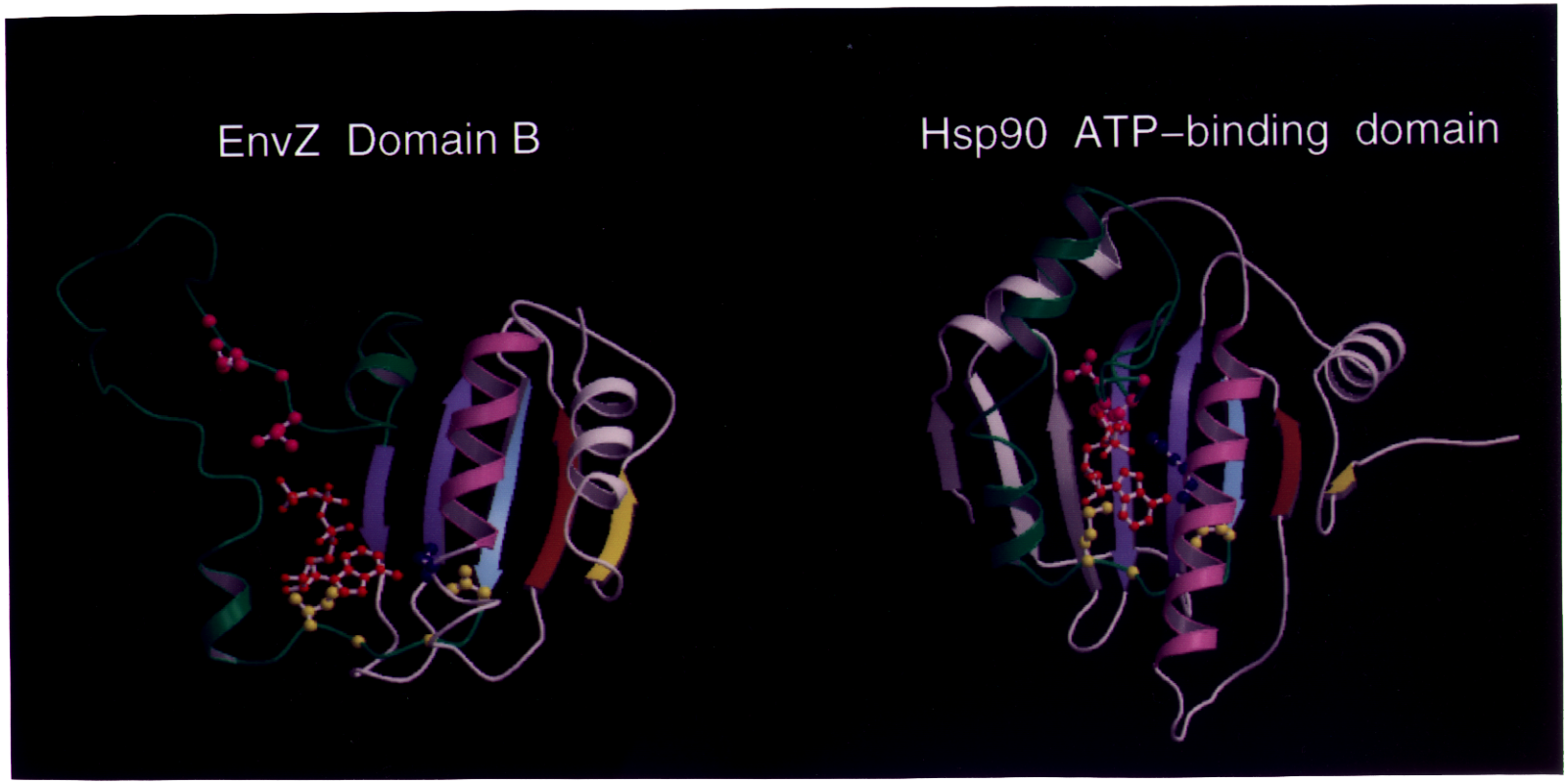

Figure II-6. Ribbon representation of domain B and the ATP-binding domain of Hsp90 molecular chaperone (PDB; 1amw).

For domain B, strand B is shown in yellow, strand D in orange, strand E in light blue, strands F and G in purple, helix α2 in pink, and the central loop including helices α3 and α4 in green. Heavy atoms (except N, C, and O) of Asn-347 (in blue), Asp-373, Gly-375, Gly-377, Ile-378 (in yellow), Gly-403, Leu-404, Gly-405, and Leu-406 (in magenta) are shown as ball-and-stick models. The corresponding secondary structural elements and specific residues of Hsp90 are colored as same with domain B. AMP-PNP (ADP in Hsp90) is also shown as ball-and-stick model in red. The model was generated using MOLSCRIPT and Raster3D.